

Article

# Silicene Quantum Capacitance Dependent Frequency Readout to a Label-free Detection of DNA Hybridization

Md. Sazzur Rahman<sup>1,†</sup> , Rokaia Laizu Naima<sup>2,†</sup>, Khatuna Jannatun Shetu<sup>3</sup>, Md. Mahabub Hossain<sup>4</sup>, M. Shamim Kaiser<sup>5\*</sup>, A. S. M. Sanwar Hosen<sup>6</sup>, Md. Abdul Latif Sarker<sup>7</sup> and Kelvin J. A. Ooi<sup>8\*</sup>

<sup>1,5</sup> Institute of Information Technology, Jahangirnagar University, Savar, Dhaka-1342, Bangladesh; {sazzad,mskaiser}@juniv.edu

<sup>2,3,4</sup> Dept of Electronics and Communicaiton Engineering, Hajee Mohammad Danesh Science & Technology University; {Rokaiyalaizu,jannatunshetu,im.mahabub}@gmail.com

<sup>6</sup> Division of Computer Science and Engineering, Chonbuk National University, Jeonju 54896, South Korea; sanwar@jbn.ac.kr

<sup>7</sup> Dept. of Electronic Engineering, Hanyang University, South Korea; abdul123@hanyang.ac.kr.

<sup>8</sup> Dept. of Physics, Xiamen University Malaysia, kelvin.ooi@xmu.edu.my

\* mskaiser@juniv.edu, kelvin.ooi@xmu.edu.my

† These authors contributed equally to this work.

**Abstract:** Two-dimensional silicon allotropes– also called Sinicene– have recently experienced intensive scientific research interest due to their unique electrical, mechanical, and sensing characteristics. A novel silicene based nano-material has been enticed great amenities, partially because of its uniformity with graphene. Silicene is a highly sensitive for numerous sensors based on molecular sensing as pH sensor, gas sensor, ion sensor and biosensing are Deoxyribonucleic acid (DNA) nucleobase sensor, photonic sensor, cell-based biosensor, glucose sensor, and bioelectric nose sensor. Nowadays genetic research based on DNA hybridization, which is a vital tools for sensing material and it has various detection methods. Among of them, the detection method is frequency readout used to a label-free detection of DNA hybridization. In this paper we have compared the graphene and silicene quantum capacitance that has been proposed for a DNA hybridization detection method on wireless readout. These method shows, the strands of mismatched and complementary DNA have in different range of frequency to identify output efficiency. With respect to DNA concentration the output of silicene is almost sharply linear than graphene. In addition of field effect transistor, silicene opens a new opportunities due to its band gap whereas graphene indicates zero band gap. It can be stated that silicene is much more reliable as well as much stronger than multi-layered graphene.

**Keywords:** Silicene; Graphene; DNA; hybridization; Biosensor; ISFETs.

## 0. Introduction

DNA hybridization computes the degree of similarity in pools of DNA sequences. Today's the identification of different deadly diseases such as hepatitis B, cancer and other complex pancreatic coronary diseases are used in DNA hybridization [1]. In biological aspect, DNA hybridization provides an enormously powerful tool that allows the identification and cloning of specific genes, analysis of the copy number of the sequence in the genome. Recent applications of DNA hybridization include the detection of human chromosomal aberrations, DNA fingerprinting, exposition of gene rearrangement and oncogene amplification in many tumors. Detection of diseases adhering gene expression by DNA hybridization is necessary diagnostic methods [2]. With exceptional properties, graphene was explained to be prominent among the material to be used in DNA sequences. Graphene based DNA hybridization sensors have been recently developed but their sensitivity is very limited. We demonstrate silicene as sensing materials instead of graphene to achieve high sensitivity. Because in real time analysis, the application of silicene nanotube-based DNA hybridization sensor provides high sensitivity, high efficiency, better tunability and lower band charge density of molecular biology [3].

Since, silicene is the silicon analogy of graphene that enabled a variety of high-performance devices ranging from linear and nonlinear circuits. The discovery and suc-

successful application of silicene, it belongs to the xenes elemental group IV that has been one of the most investigated materials in physics and nanoscience [4,5]. In 1994, silicene was first demonstrated a 2D material that is arise silicon as “Silic” and “ene” from graphene. The physical property of free standing silicene with spin orbit band gap of 1.55 meV, that is much higher than graphene [6]. Experimental evidence of silicene, the graphene analogy of silicon, has open ground breaking opportunities to the theoretical and experimental physicist [7].

With atomic resolution, silicene nano wires and silicene sheets have been grown on silver crystal as Ag (110) and Ag (111) [8]. Since its invention, it has numerous properties such as physical and electrochemical. Silicene has high intrinsic mobility ( 1000 cm<sup>2</sup>/Vs) at room temperature [9], a better tunability of band gap (0.50 eV) which is necessary for field effect transistor (FET) [10,11], high speed switching, and a much stronger spin orbit coupling. In Silicene, FET requires a large supply voltage about 30 V to turn on and band gap down to 0.1 eV [12]. The sensing material of silicene that provides high efficiency, and lower its carrier density due to strong silicene trail for high performance FETs, large band gap, high Fermi velocity (5.2105 m-S) [13]. These advantages made silicene an endurable fluidity for chemical and biological sensing that can be mobilized with nano electronics technology [14]. With compare to graphene, silicene has sp<sup>3</sup> hybridization instead of sp<sup>2</sup> hybridization that is conduct to potential interaction including exterior particles. For active conduction of atomic sensing, silicene is a promising material that is used in molecular detection technique [15]. Therefore, applying these materials is used to supervise DNA sequencing of silicene nano-pore [16].

In this paper, we introduce the concepts of frequency readout to a label free detection of DNA hybridization. Sensing on silicene surface, if quantum capacitance changes, it will change the carrier concentration. Therefore, quantum capacitance also changes with DNA hybridization. DNA strands are negatively charged, hybridization makes it more negative. Therefore, the carrier concentration changes with hybridization. We proposed the physical, analytical and simulation results of silicene that state the implementation of DNA hybridization will effectively enhance the sensors activity. Also, it will decrease the difficulties of numerous experimental analyses. The contribution of the work is summarized as bellow:

- We have studied a broad range of biochemical sensors that offer fast, simple and inexpensive real time analysis of DNA hybridization.
- We have performed a comparative study to find out the most efficient and flexible scheme in silicene quantum capacitance with the help of a RLC circuit-based system modeling.
- We have used wireless sensors for points of care diagnostics due to its superconductivity.

The remaining of this paper is outlined as follows. Section 1 studied the analytical method of silicene and graphene quantum capacitance. The DNA hybridization and design principles are simplified in Section 2. The system model of DNA hybridization detection and pH detection are described in Section 3. The performance of silicene and graphene quantum capacitance in terms of frequency readout is presented in Section 4. The concluding remarks are provided in Section 5.

## 1. Analytical Method of Silicene and Graphene Quantum Capacitance

Many RLC systems are based on resonator circuit, which consists of different semiconductor devices such as resistors, inductors and capacitors operate as resonant frequency. While silicene, the quantum capacitance based wireless sensor that is connected with an inductor then the resonant frequency will change. Since the quantum capacitance is changed with DNA hybridization, an RLC circuit can be used as a DNA hybridization sensor. Applied in DNA hybridization sensor this device make silicene scheme must be proceed and varies carrier concentration.

In silicene quantum capacitance ( $C_{Q1}$ ) is defined by Eq. 1 that has been expressed in

[17].

$$C_{Q1} = \frac{2e^2kT}{\pi(hv_F)^2} \times \ln \left[ 2 \left( 1 + \cosh \frac{E_F}{kT} \right) \right] \times (L_g W_g N). \quad (1)$$

Here,  $e$  is the charge of electron,  $k$  is the Boltzmann constant,  $T$  is the temperature in Kelvin,  $v_F$  is the Fermi velocity,  $h$  is the Planck's constant,  $E_F$  is the Fermi energy level,  $L_g$  and  $W_g$  are the length and width of each gate respectively,  $N$  is the number of fingers.

If  $E_F \gg kT$ , then Eq. 2 can be modified as below

$$C_{Q1} = \frac{2e^2}{(hv_F)\sqrt{\pi}} \sqrt{n} (L_g W_g N), \quad (2)$$

where  $n$  is the net carrier concentration. In silicene device, carrier concentration can be define as  $n = |n_G| + |n^*|$  where  $n_G$  is the carrier concentration  $n_G = (\frac{eV}{hv_F\sqrt{\pi}})^2$  and  $n^*$  external charge on silicene surface.

The device's gate capacitance is equal to oxide capacitance in series with quantum capacitance. The gate capacitance is given by Eq. 3

$$\frac{1}{C_G} = \frac{1}{C_{OX}} + \frac{1}{C_Q}, \quad (3)$$

where  $C_{OX}$  is the oxide capacitance as in Eq. 4

$$C_{OX} = 3.9 \times \frac{\epsilon_0}{EOT} (L_g W_g N), \quad (4)$$

where  $\epsilon_0$  is the permittivity of free space and EOT denotes the equivalent oxide thickness.

The resonant frequency of  $L$  and  $C_G$  of the device can be expressed as in Eq. 5.

$$f = \frac{1}{2\pi\sqrt{LC_G}}. \quad (5)$$

The  $C_{Q1}$  or gate capacitance ( $C_G$ ) can be defined as in Eq. 6.

$$C_G = \epsilon_0 \epsilon_r \frac{L_g W_g}{t_{OX}}, \quad (6)$$

where  $\epsilon_0 \epsilon_r$  is the dielectric constant ( $8.85 \times 10^{-12}$ ) F/m (Farad per meter) and  $t_{OX}$  is the oxide thickness of gate dielectric in nm.

To introduce a conceptual prognosis of quantum capacitance  $C_Q$  for ideal graphene, can be expressed [18] as the form of Eq. 1

$$C_Q = \frac{2e^2kT}{\pi(hv_F)^2} \times \ln \left[ 2 \left( 1 + \cosh \frac{eV_{ch}}{kT} \right) \right], \quad (7)$$

where the fermi velocity of the dirac electron  $v_F = c/300$  and  $V_{ch} = EF/e$  is the potential of graphene.

$$C_Q \approx e^2 \frac{2eV_{ch}}{\pi(hv_F)^2} = \frac{2eV_{ch}}{\sqrt{\pi}(hv_F)^2} \sqrt{n}. \quad (8)$$

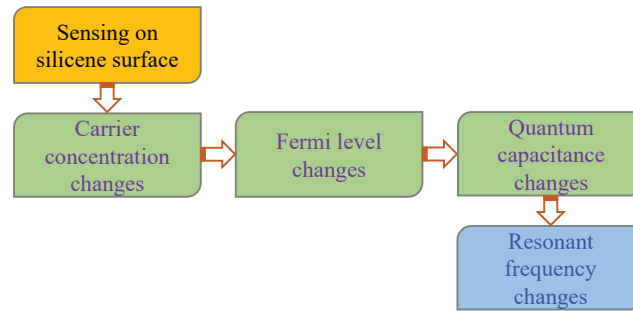


**Figure 1.** Transduction method of silicene quantum capacitance based frequency readout.

Emerging in silicene quantum capacitance based wireless sensor, the conduction process are delineated in Fig 1. An electrochemical substrate was used in this mechanism. When selecting a substrate for electrochemical applications, the electrochemical reactivity of the substrate is an important criterion to consider [19]. In chemistry, a substrate is typically the chemical species observed in a chemical reaction which react with a reagent to generate a product. Then  $SiO_2$  surface has been used for sensing on silicene. When sensing on silicene surface we used DNA hybridization sensor that are useful to detect wireless readout. After sensing on silicene surface, it will change the carrier concentration. The carrier concentrations are also change the Fermi velocity. After changing the Fermi level velocity it changes the quantum capacitance and the quantum capacitance also change the resonant frequency. Then the transaction mechanism can perform the quantum capacitance of frequency readout.

## 2. Design Principle

The basic detection principles of biochemical sensors that have been employed for DNA hybridization detection methods which convey the necessary information. DNA hybridization is the biochemical reaction which brings to the formation of double helix structure from two single stranded, complementary DNA strands. In electrochemical substrate, the executed responses that are produces from charge  $\sigma_0$  which is remaining at the sensing surface.

As shown in the Figure 2, the capacitance is submitted as a series combination of double layer, denoted by  $C_{DL}$ , and FET sensor capacitance, denoted by  $C_{FET}$ , respectively. The  $C_{FET}$  can be expressed as

$$\frac{1}{C_{FET}} = \frac{1}{C_b} + \frac{1}{C_{OX}} \quad (9)$$

where  $C_{OX}$  is the gate oxide capacitance and  $C_b$  depletion capacitance. The value of  $C_b$  is the smaller and determines the overall sensor capacitance. The potential  $\psi_0$  due to chemical reaction of the surface can be given as Eq.10 [20].

$$\psi_0 = \frac{\Delta\sigma_0}{C_{DL} + C_{FET}}, \quad (10)$$

The transistor biasing depends on either of these capacitances that can be bringing under control. Field effect transistor in Ion Sensitive FET (ISFET), the equations can be expressed as Eq. 11.

$$I_{DS} = \frac{\mu C_{OX} W}{L} [(V_{GS} - V_{th}) V_{DS}] - \frac{V_{DS}^2}{2}. \quad (11)$$

Given,

$$V_{th} = \frac{\phi_m - \phi_s}{e} - \frac{Q_i}{C_{OX}} - \frac{Q_B}{C_{OX}} - 2\phi_F, \quad (12)$$

where  $\phi_F$  is defined as channel effects of the channel and

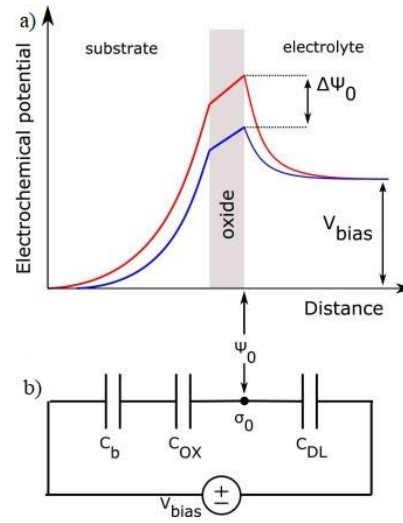


**Figure 2.** a) A simplified model of electrochemical cell, and b) Equivalent circuit of the sensor.

$$\phi_F = E_{ref} + \chi_{sol} - \psi_0, \quad (13)$$

here,  $E_{ref}$  is the potential difference between liquid and reference electrode of the surface,  $\chi_{sol}$  is the surface dipole potential of the solution,  $\psi_0$  is the surface potential which results from the chemical reaction.

Hybridization is a sequence of class of methods for determining the order of DNA strand which typically used for looking an inconsiderable change is comparatively known as DNA sequence. The two sequences A and B of this process are single-strand probe DNA (ssDNA) that indicates on complementary DNA or mismatched DNA which is referred as target probe DNA. This complement produces the results of entirely matched double-strand probe DNA (dsDNA) which perform hybridization. After initialization, compute the minimum length of two DNA sequence. If the two input DNA probes are equal then the matched DNA are increases there after the sub matrix of two sequences are calculated. The resultant value is then increment one by one then compares the length of DNA probe. If the length is greater than the incremented value, then the loop is continuously updating the performance. Otherwise it displays the output score. On the other hand, the sequences of two DNA probe are different then calculated the mismatched DNA which increases the mismatch count and produces the results of output score. When the counter is less than the probe length then sequentially produces the output of the sequences.

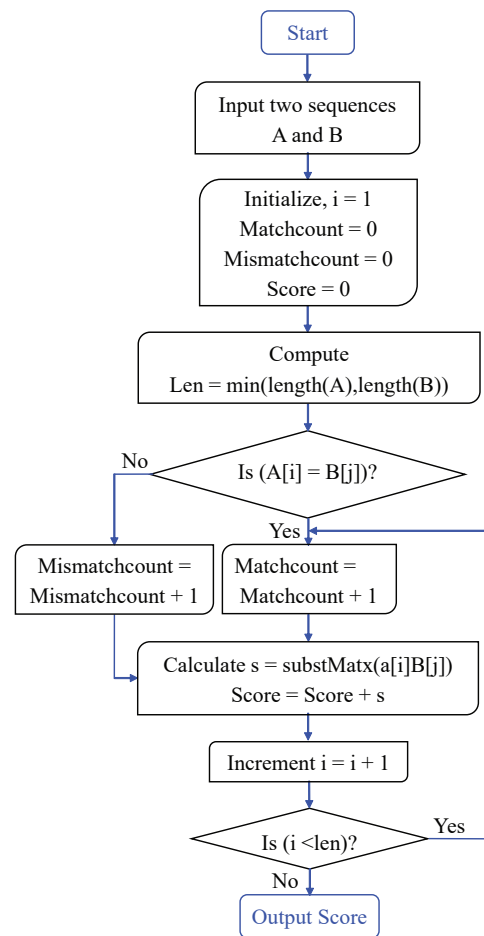


**Figure 3.** Flowchart of DNA hybridization in two samples.

### 3. System Model based on Detection Principle

#### 3.1. DNA hybridization process

The information attained from the DNA samples are corresponding to produces DNA-DNA probes that are target analysts. The DNA-DNA probes are performing antigen-antibody layer of different ions that are generated such as  $H^+$ ,  $Na^+$ , and  $K^+$  by using ion-selective membrane. After executing these ions are performing the enzyme reaction layer. The enzyme reaction layers are produces analyst and product enzyme. These initializing steps are performing the recognition layer then send to transducer. Through, field effect transistor the transducer converts an electrical signal. Depending on the electronic system applications, the electrical signal can be amplified processed and then displayed or send to the display [21]. This process is shown in Fig. 4.

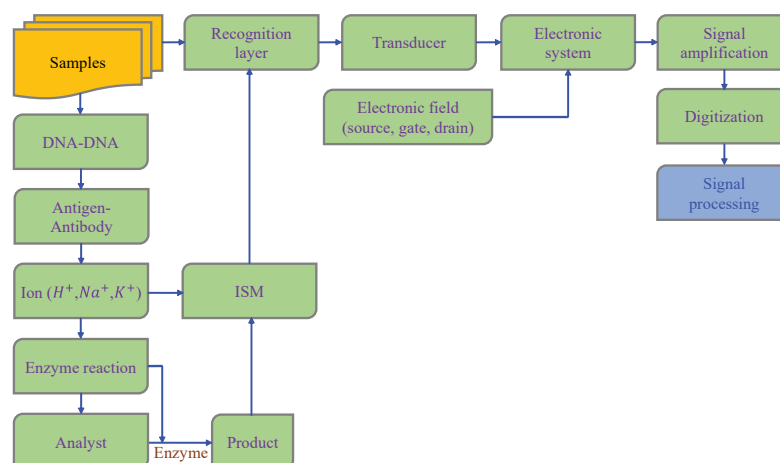


**Figure 4.** DNA hybridization process.

The appropriate DNA detection techniques are based on DNA-based analytical method that are most established, sensitive, qualitative, quantitative, real time analysis.

The DNA-DNA sample of ions are design to facilitate the conventional ion selective electrode (ISE) based on internal repletion analysis in combination with an ion-selective membrane (ISM). To compare with traditional ISE layer, the achievement of ISM output is smaller, simpler, accessible, and robust. Using a high-impedance voltmeter, the potential of the electrode is adequate contrary to a reference electrode. Due to zero current condition, there is no ohmic potential drop, if it conducts ideally in the system.

### 3.2. pH Detection Model

The biosensors have attract a great attention by the researchers due to fast and reliable application [22]. To achieve more robust sensing, it is necessary to demand more fabricated specimen formulation and assessment scheme. The samples can be consists of various important target analysts that can be used to detect of DNA hybridization. For the multiplexed detection of DNA hybridization, a number of targets in a single reaction are better suited. With different DNA probes, the process of the function is acquired by organize various transistors in a single array [23]. In pH scale identification of DNA hybridization applying the electro-static repulsion within DNA probe and target DNA is allayed, and hybridization may be accomplished in lower salt concentration. For determining ion-concentrations in pH scale solution, that used an ion-sensitive field effect transistor. When the current through the transistor that will changes seen in pH scale, the ion concentrations of  $H^+$  also changes consequently [24]. Where, the solution of ion concentration is performed as the gate electrode. The Fig. 5 illustrates the analysis of pH detection model.

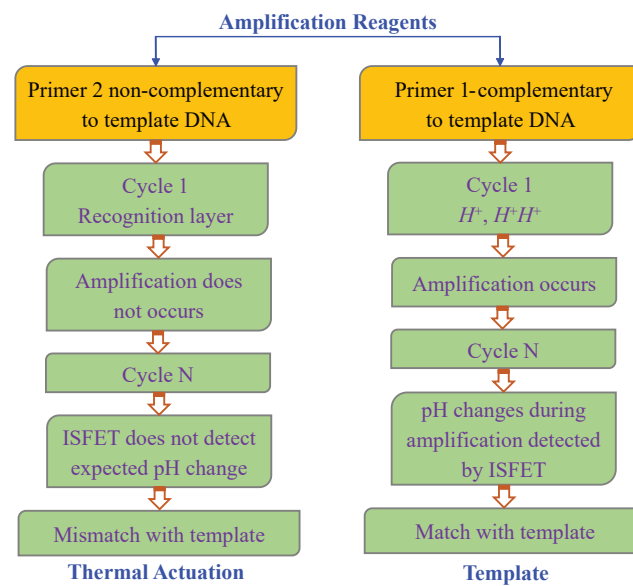


**Figure 5.** The model of pH detection.

The process of DNA amplification that fair  $H^+$  wherein nucleotides are organized to rising duplicate strands DNA. This chemical reaction is detected using ISFETs. By applying a gate voltage, the chemical reaction at the surface of the oxide will change the charge density on the channel. Thus, the induced charge density in the channel of the FET will be changed. As a consequence, the drain to source current  $I_{DS}$  will be changed as a function of the pH at the interface of the  $SiO_2$  surface for sensing on silicene. The template of DNA sequencing device, amplification reagents and the thermal actuation combinations are performed complementary and non-complementary probe. In complementary DNA template are produces  $H^+$  ions and amplification occur that produced double  $H^+$  ions. The ion sensitive field effect transistors are changes pH and amplification is detected that are match with template. So, pH is detected with DNA hybridization. On the other hand, in the case of non-complementary DNA template does not produce  $H^+$  and no amplification occur. The cycle does not hybridize. Therefore, the ion sensitive field effect transistor does not detect the expected pH change which is mismatch with sequencing reagents.

#### 4. Experimental Analysis and Results

##### 4.1. Experiment Setup

This section compares the performance of silicene and graphene in terms of frequency readout. This analysis takes into account the average frequency. The quantum capacitance is affected by carrier concentration when DNA hybridization changes. In addition, the DNA hybridization changes the carrier concentration. The quantum capacitance of the devices' silicene channel changes as the carrier concentration changes.

**Table 1.** Parameters and values for silicene.

Parameter	Value
Gate length	$1 \mu m$
Intrinsic mobility	$1000 cm^2/Vs$
Oxide thickness	$6 \text{ \AA}$
Fermi velocity	$5.21 \times 10^5 ms^{-1}$
Band gap	$0.50 eV$
Quantum capacitance	$0.1475 \times 10^{-12} F$



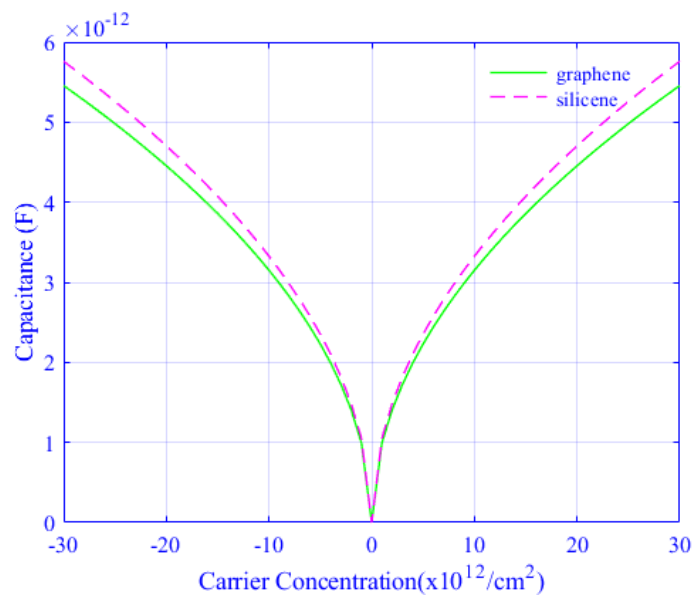
**Table 2.** Nominal Parameters and values for Graphene [26].

Parameter	Value
Gate length	$0.2\mu m$
Extension length	$0.1\mu m$
No. of finger	200
Mobility (both $e$ and $h$ )	$400cm^2/Vs$
Finger width	$10\mu m$
Temperature	$300k$
Gate finger pitch	$0.6\mu m$
Gate length	$0.2\mu m$

The silicene channel of the scheme is associated to inductor that invents a resonant circuit. The quantum capacitance and oxide capacitance are connected in series and due to the smaller value of quantum capacitance, it determine the total capacitance. The total capacitance plays role to change the resonant frequency of the devices.  $f = 1/(2\pi\sqrt{LC_G})$  is the general equation of resonant frequency. Where,  $L$  is defining as an inductor and  $C_G$  is the gate capacitance of resonant circuit. To compare between the aforementioned schemes are evaluated for different pulse of frequency regarding to quantum capacitance for different inductor values; i.e,  $L = 250 nH$  as Blue,  $L = 2.5 \mu H$  as Red,  $L = 25 \mu H$  as Green. With the use of MATLAB tools, simulation has been done and the results are presented for an ideal channel with no other distortion. The simulation was carried out by considering the parameters that are shown in Table I and Table II for ideal silicene and graphene channel of the devices, respectively.

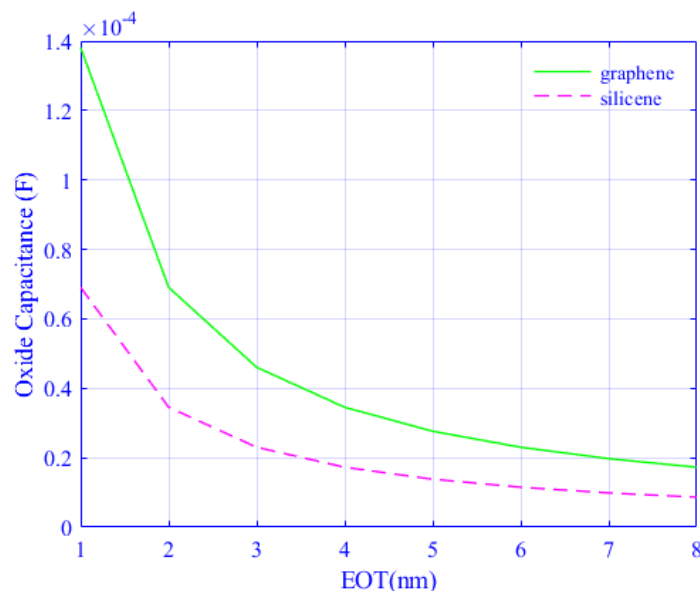
#### 4.2. Performance Metrics

The simulated results for all the schemes of silicene are represented by lines with markers (Red), while that of the graphene are marked by solid lines (Blue). The Eq. (2) and Eq. (9) exhibits the familiarity within quantum capacitance and carrier concentration of graphene and silicene channel of the devices, respectively, and their performances are shown in Fig. 6. For the case of graphene, the modulus of the carrier concentration varies from  $0.30 \times 10^{12}/cm^2$  and the corresponding quantum capacitance decreases from  $5.5 pF$  to 0 for the negative carrier concentration and it increases from 0 to  $5.5 pF$  for the positive carrier concentration. As well as for silicene, the behavior of the quantum capacitance variation with carrier concentration is similar to that of graphene except the peak value of quantum capacitance is  $5.8 pF$  which is much sharper than graphene. When we measure the quantum capacitance versus carrier concentration of label free DNA hybridization, we get quantum capacitance up to  $5.8 pF$  for silicene which is appreciable. It may conclude that carrier concentration is more sensitive with silicene quantum capacitance than graphene.



**Figure 6.** The effect of carrier concentration ( $30 \times 10^{12}/\text{cm}^2$ ) on Quantum capacitance for both silicene (dotted line) and graphene (solid line).

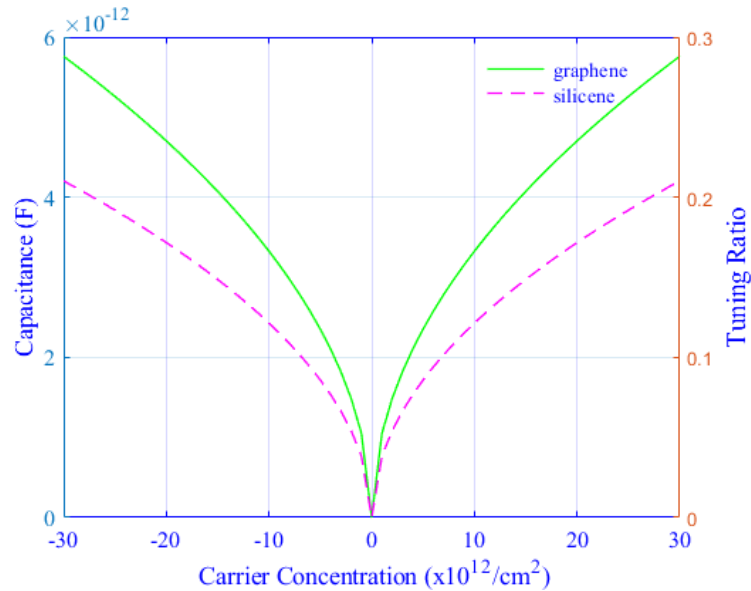
Fig. 7 shows the oxide capacitance as a function of Effective Oxide Thickness (EOT) which is relay on the area of gate oxide thickness. The channel of the device capacitance depends on the EOT when the device gate area is fixed. From figure it is found that with the increasing of the effective oxide thickness the oxide capacitance decreases exponentially for both the cases of silicene and graphene. With the variation of the EOT from 1 nm to 8 nm, the oxide capacitance decreases for both of the graphene and silicene from 14 mF to 1.9 mF and 6.5 mF to 1.5 mF, respectively, while the quantum capacitance was kept maximum for both cases.



**Figure 7.** Oxide capacitance decreases with. Effective Oxide Thickness (EOT) (nm) for both silicene (dotted line) and graphene (solid line)

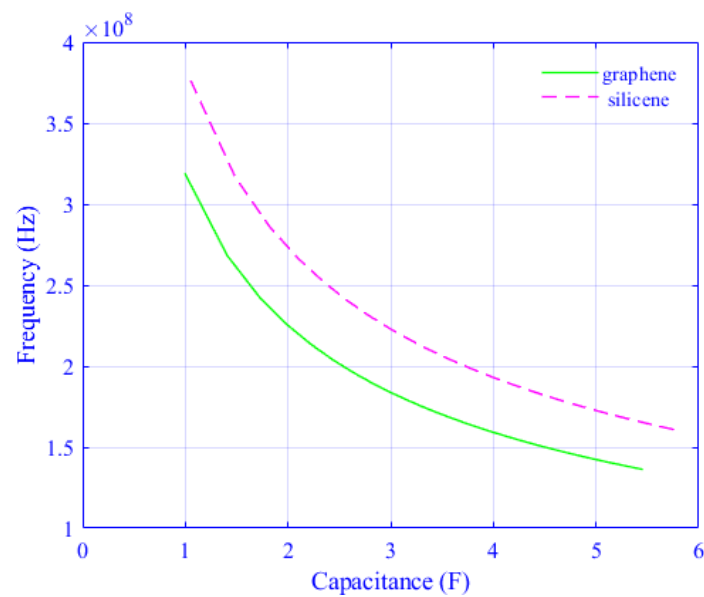
Fig. 8 represents the capacitance and tuning ratio as a function of carrier concentration for silicene and graphene. The graph can be divided into halves in X-axis to explain the characteristics of the graph properly. The first and second halves are considered as a function of the carrier concentration from  $-30 \times 10^{12}/\text{cm}^2$  to 0 and 0 to  $30 \times 10^{12}/\text{cm}^2$ ,

respectively. Both the capacitance and tuning ratio decreases sharply for the negative carrier concentration (the first half) whereas the capacitance and tuning ratio increases rapidly for the positive carrier concentration (the second half). The peak value of the capacitance and tuning ratio of the channel is  $5.8 \text{ pF}$  and  $0.2$ , respectively.



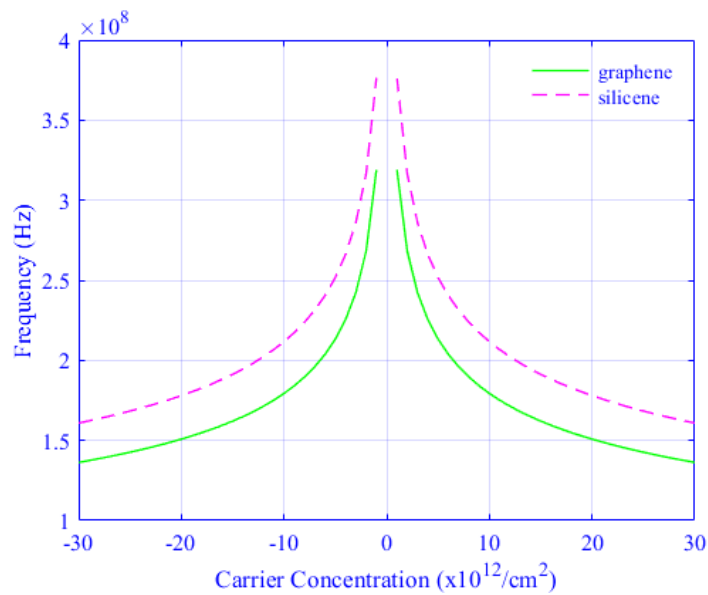
**Figure 8.** Effect of carrier concentration on the capacitance and tuning ratio for both silicene (dotted line) and graphene (solid line).

The resonant frequency depends solely on the channel of the inductor. At zero gate voltage the value of inductor,  $L \approx 250 \text{ nH}$  was ascertain conduct frequency  $f = 1 \text{ GHz}$ . Through the increment of the inductor values ( $L = 250 \text{ nH}$ ,  $L = 2.5 \text{ } \mu\text{H}$  and  $L = 25 \text{ } \mu\text{H}$ ), the resonant frequencies are decreased. Fig. 9 displays the relationship within the frequency and capacitance of graphene and silicene at a constant value of  $L$ . The X-axis represents the values of capacitance within the range from  $1 \times 10^{-12}$  to  $6 \times 10^{-12} \text{ F}$  and the Y-axis represents the frequency within the range from 0 to  $4 \times 10^8 \text{ Hz}$ . With the increases of the capacitance, the frequency decreases exponentially for the both of graphene and silicene. Each of those graphs show the frequency is at  $(.1 \text{ } 1) \text{ GHz}$  for inductor values are  $L = 250 \text{ nH}$  and  $L = 2.5 \text{ } \mu\text{H}$  and  $L = 25 \text{ } \mu\text{H}$ , as a consequence of frequency and capacitance are  $3.8 \times 10^8 \text{ Hz}$  and  $5.8 \times 10^{-12} \text{ F}$  for silicene while that values are  $3.3 \times 10^8 \text{ Hz}$  and  $5.5 \times 10^{-12} \text{ F}$ , respectively for graphene.



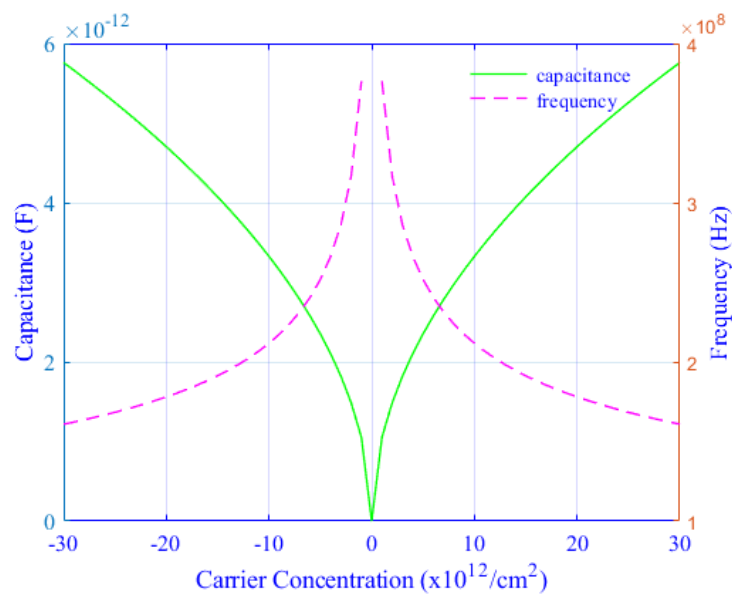
**Figure 9.** Frequency (Hz) decreases with the capacitance ( $\times 10^{-12}F$ ) for both silicene (solid line) and graphene (dotted line).

Fig. 10 illustrates the carrier concentration has significant effect on the capacitance and frequency for silicene and graphene. The resonant frequency has achieved at the inductance of 250 nH. The graph again can be divided into halves in X-axis to explain the characteristics of the graph properly. The first and second halves are considered as a function of the carrier concentration from  $-30 \times 10^{12}/cm^2$  to 0 and 0 to  $30 \times 10^{12}/cm^2$ , respectively. For the both cases, the frequency increases very rapidly for the negative carrier concentration (the first half) whereas the frequency decreases very sharply for the positive carrier concentration (the second half). The minimum and maximum frequencies are  $1.6 \times 10^8$  Hz and  $3.8 \times 10^8$  Hz, respectively, for silicene and that values are  $1.4 \times 10^8$  Hz and  $3.2 \times 10^8$  Hz, respectively, for graphene. It is observed from the Fig. 9 that the change of frequency with respect to the carrier concentration for silicene is sharper than that of the graphene. It is also found that the peak amplitude of the frequency for silicene is higher than that of the graphene. Therefore, it is evident from the Fig. 9 and Fig. 10, silicene are more sensitive than graphene as a sensing material.



**Figure 10.** Effect of carrier concentration on the capacitance for both silicene (dotted line) and graphene (solid line).

Fig. 11 illustrates the carrier concentration has significant effect on the capacitance and frequency for silicene. The graph can be divided into halves in X-axis to explain the characteristics of the graph properly. The first and second halves depends on the carrier concentration from  $-30 \times 10^{12}/\text{cm}^2$  to 0 and 0 to  $30 \times 10^{12}/\text{cm}^2$ , respectively. The X-axis represents the values of capacitance within the range from  $0$  to  $6 \times 10^{-12}$  Farad and the Y-axis represents the frequency within the range from  $1 \times 10^8$  to  $4 \times 10^8$  Hz. In negative carrier concentration (the first half) the capacitances are decreases with the frequency are increases. Whereas in positive (the second half) carrier concentration the capacitance increases when the frequency decreases. So, the frequency and capacitance are inversely proportional to carrier concentration and the value of capacitance is maximum at  $5.8 \times 10^{-12}$  Farad and the frequency  $1.6 \times 10^8$  Hz. In above Figs. 9, 10 and 11, we concluded that when the value of carrier concentration are positively or negatively increases that increases the capacitance. But when the carrier concentrations are positively or negatively decreases then the frequency are decreases. So, the carrier concentration is proportionally changed with capacitance and frequency, and the sensitivity of silicene is much more effective than multilayer graphene.



**Figure 11.** Effect of carrier concentration on the capacitance as well as frequency.

#### 4.3. Limitations and Future

Concerning the last several decennary, empirics have been concentrated on flourishing sensors including ultra low limits of detection. In consequence, an extensive spread of schemes with various functional modalities has been exhibited. The sensor of carbon materials has high sensibility and high efficiency that has been attained. Nevertheless, there are a number of objections for identifying low concentration of DNA analytical method of sequencing probe.

The improvements of SNR (signal to noise ratio) of channels are mostly depending on the deficiency of DNA concentration which becomes an emergent mission. To optimistic operational settings of carbon based devices required necessary effort for DNA hybridization. Silicene is also a fascinating to hunt for the channel that approves the identification of a single DNA hybridization strand. On the basis of device structure and the formation of carbon components the electrical detection of DNA hybridizations are exceedingly reclines. Therefore, the identification of DNA hybridization is rapid, specific, and low cost which could speed up the performance. Silicene based devices have demonstrated the extensive efficient for the posterior applications of DNA biosensors.

## 5. Conclusions

The 2D material of silicene is used in highly sensitive molecular sensors that have lower charge density than graphene. Silicene does have a band gap which makes it suitable to be used in novel transistors and others. We use the various detection principles of biochemical and electrochemical sensors that convey the necessary information for detection of DNA hybridization.

The comparison between silicene and graphene was performed based on the RLC circuit modeling and thus via the resonant frequency of the system. In presence of silicene channel device, it is shown that when the carrier concentration is increased, the capacitance is also sharply increased compared to graphene. The frequency response is nearly linear as regards to DNA concentration. Therefore, to continue the operating performance, the device of material sensing of silicene is added to label free detection of DNA hybridization which demonstrated the frequency readout of the systems. .

**Author Contributions:** Conceptualization, MSR and RLN; methodology, MSR, RLN, KJS and MMH ; software, MSR, RLN; validation and formal analysis, MSK, ASMSH, MALS and KJAO; writing—MSR, RLN and KJS; writing—review and editing, MMH, MSK and ASMSH; visualization, MSR and RLN. All authors have read and agreed to the published version of the manuscript.

**Funding:** “Xiamen University Malaysia Research Fund, grant no XMUMRF/2019-C3/IECE/0003”

**Institutional Review Board Statement:** No ethical approval required.

**Informed Consent Statement:** Not applicable

**Acknowledgments:** In this section you can acknowledge any support given which is not covered by the author contribution or funding sections. This may include administrative and technical support, or donations in kind (e.g., materials used for experiments).

**Conflicts of Interest:** The authors declare no conflict of interest.

## Abbreviations

The following abbreviations are used in this manuscript:

cDNA	Complementary DNA
DsDNA	Double-strand DNA
DNA	Deoxyribonucleic Acid
EOT	Effective Oxide Thickness
EOT	Effective Oxide Thickness
FET	Field Effect Transistor
GNR	Graphene Nano-ribbon
ISE	ion selective
ISFET	Ion -sensitive FET
ISE	Ion-selective electrode
ISM	Ion-selective membrane
RLC	Resistor inductor and capacitor circuit
ssDNA	Single-strand-DNA
SiNR	Silicene Nano-ribbon
SNR	Signal-to-noise ratio
SiNW	silicon nanowires
2D	Two Dimensional

## References

- Huang, C.W.; Huang, Y.J.; Lin, T.H.; Lin, C.T.; Lee, J.K.; et al. An integrated microcantilever-based wireless DNA chip for Hepatitis B Virus (HBV) DNA detection. In *Proc. of the 15th International Conference on Miniaturized Systems for Chemistry and Life Sciences (MicroTAS'11)*, Seattle, Washington, USA, 2011; 984–986.
- Manoharan, A. K.; Chinnathambi, S.; JayavelR. Simplified Detection of the Hybridized DNA Using a Graphene Field Effect Transistor. *Science and Technology of Advance Materials* **2017**, *18(1)*, 43–50.
- Salimian, F.; Dideban, D. A. Silicene Nanotube Field Effect Transistor (SiNTFET) with an Electrically Induced Gap and High Value of  $I_{on} / I_{off}$ . *ECS J. Solid State Sci. Technol.*, **2018**, *7*.
- Molle, A.; Goldberger, J.; Houssa, M.; Xu, Y.; Zhang, S.; Akinwande, D. Buckled two-dimensional Xene sheets. *Nature Materials*, **2017**, *16(2)*, 163–169.
- Vogt, P; Padova, D P; Quaresima, C; Avila, J; Frantzeskakis, E; et al. Silicene: Compelling Experimental Evidence for Graphene like Two-Dimensional Silicon. *Physical review letters*, **2012**, *108(15)*, 155501/1–5.
- Liu, C.; Feng, W.; Yao, Y. Quantum spin Hall effect in silicene and two dimensional germanium. *Physical review letters* **2011**, *107*, 706–802.
- Cahangirov, S.; Sahin, H.; Lay, G. L.; Rubio, A. Introduction to the Physics of Silicene and other 2D Materials. *Lecture Notes in Physics*, **2017**, *930*.
- Zhuang, J.; Xu, X.; Feng, H.; Li, Z.; Wang, X; Du, Y. Honeycomb Silicon:A review of Silicene. *Science Bulletin*, **2015**, *60(18)*, pp.1551-1562.
- Tao, L.; Cinquanta, E.; Chiappe, D.; Grazianetti, C.; Fanciulli, M.; et al. Silicene Field-Effect Transistors Operating at Room Temperature. *Nature Nanotechnology* **2015** *10(3)* 227–231.
- Quhe, R. Tunable Band Gap in Silicene and Germanene by Surface Adsorption. *Nano Lett.* **2012** *2(853)* 113–118.
- Quhe, R.; Fei, R.; Liu, Q.; Zheng, J.; Li, H.; et al. 2012. Tunable and sizable band gap in silicene by surface adsorption. *Scientific reports*, **2012**, *2(1)*, 1-6.
- Ni, Z.; Zhong, H.; Jiang, X.; Quhe, R.; Luo, G.; et al. 2014. Tunable band gap and doping type in silicene by surface adsorption: towards tunneling transistors. *J. Nanoscale* **2013** *6(13)* 7609–7618.
- Roome, N. J. et al. Beyond Graphene:Stable Elemental Monolayer of Silicene and Germanene. *ACS Applied Materials & Interfaces* **2014** *6(10)*.

14. Luan, H.; Zhang, C.; Li, F.; Wang, P. Electronic and Magnetic Properties of Silicene Nanoflakes by First-principles Calculation., *Physics Letters A* **2013** 377 2792–2795.
15. Aleshaikh, S.; Shahtahmassebi, N.; Roknabadi, M. R.; Shahri, R. P. Silicene Nanoribbon as a New DNA Sequencing Devices. *Physics Letters* **2018** 382, 595–600.
16. Sadeghi, H.; Bailey, S.; Lambert, C. J. Silicene-based DNA Nucleobase Sensing. *Applied Physics Letters* **2014** 104, 103–104.
17. Fang, T.; Konar, A.; Xing, H. Carrier statistics and quantum capacitance of graphene sheets and ribbons. *Applied Physics Letters* **2007** 91, 92–109.
18. Tao, M.; Xia, J. Measurement of the Quantum Capacitance of Graphene. *Journal of Nanoscience and Nanotechnology* **2009** 117, 505–509.
19. Benck, J. D.; Pinaud, B. A.; Gorlin, Y.; Jaramillo, T. F. Substrate Selection for Fundamental Studies of Electrocatalysts and Photoelectrodes: Inert Potential Windows in Acidic, Neutral, and Basic Electrolyte. *PLOS ONE* **2015** 10(4).
20. Shoorideh, K.; Chui, C. O. On the Origin of Enhanced Sensitivity in Nanoscale FET-Based Biosensors *Proceedings of the National Academy of Sciences* **2014** 111, 5111–5116.
21. Zhang, A.; Zheng, G.; Lieber, C. M. On the Origin of Enhanced Sensitivity in Nanoscale FET-Based Biosensors *In: Nanowires. NanoScience and Technology* **2016**, 255-275.
22. Hahn, S.; Mergenthaler, S.; Zimmermann, B.; Holzgreve, W. Nucleic acid based biosensors: The desires of the user. *Bioelectrochemistry*, **2005** 67, 151–154.
23. Toumazou, C., Shepherd, L.M., Reed, S.C., Chen, G.I., Patel, A., Garner, D.M., Wang, C.J.A., Ou, C.P., Amin-Desai, K., Athanasiou, P. and Bai, H., 2013. Simultaneous DNA amplification and detection using a pH-sensing semiconductor system. *Nature methods*, **2013** 10, 641–646.
24. Bergveld, P. Development of an ion-sensitive solid-state device for neurophysiological measurements. *IEEE Transactions on Biomedical Engineering*, **1970**, 7, 70-71.
25. Deen, D.A.; Olson, E.J.; Ebrish, M.A.; Koester, S.J. Graphene-based quantum capacitance wireless vapor sensors. *IEEE Sensors Journal*, **2013**, 14, 1459–1466.
26. Koester, S.J. High quality factor graphene varactors for wireless sensing applications. *Applied Physics Letters*, **2011**, 99, 163105.